TID-4500, UC-53
Meteorology

LAWRENCE LIVERMORE LABORATORY
University of California/Livermore, California/94550

UCRL-51328

AN INVESTIGATION OF SCAVENGING OF RADIOACTIVITY FROM NUCLEAR DEBRIS CLOUDS: RESEARCH IN PROGRESS

W. K. Crandall
C. R. Molenkamp
A. L. Williams
M. M. Fulk
R. Lange
J. B. Knox

MS. date: January 17, 1973

GG-

Contents

AN INVESTIGATION OF SCAVENGING OF RADIOACTIVITY FROM NUCLEAR DEBRIS CLOUDS: RESEARCH IN PROGRESS

Abstract

The publication Potential Exposures from Low-Yield Free Air Bursts, addressed the problem of rapid deposition of radioactivity from nuclear debris clouds at various distances from ground zero. The results showed that large values of infinite exposure and large exposure rates could occur at the surface under the following special circumstances: the radioactivity is distributed in the lower troposphere, it is scavenged at an early time by a rain-bearing system and rapidly deposited over the ground, and it is confined to a relatively small area. More recent studies have been and are being made at LLL to make it possible to assess 1) the reasonability of the results of this earlier publication by considering in greater detail the physical processes involved and 2) the extent to which the results may be changed by man-made modifications. This paper is a progress report on the research projects currently underway at LLL which are directed toward quantifiable assessments for client needs. Specifically, these projects are:

1) A study of the dynamics of cumulus cloud interaction with a nuclear debris cloud to determine possible enhancement or reduction in peak surface concentrations.
2) A study of the microphysical interactions of debris particles with cloud droplets and raindrops to determine rainout and washout efficiencies.
3) A study to determine the feasibility of rendering the debris particles non-wettable, thereby effectively making the rainout coefficient negligibly small.
4) A study of the potential effects of dry deposition due to the detonation of larger numbers of low yield devices within a confined area.
5) The development of a three-dimensional atmospheric diffusive particle-in-cell code capable of calculating the time-dependent distribution of air pollutants under conditions of turbulent diffusion and wind shear.

Introduction

A major conclusion from the report Potential Exposure from Low-Yield Free Air Burst[1] was that the hazard of close-in exposure from these bursts may be appreciable when scavenging by precipitation occurs. For example, rainout of the radioactivity within the debris cloud of a 1-kt nuclear detonation at 100 km downstream of ground zero may result in external gamma dose rates as high as

100 R/hr and infinite whole body doses of 1000 R or higher. A study by Conner and Phillips[2] further substantiates the hazard inherent in these low-yield bursts.

From the interest generated by these papers, it has become apparent that a greater effort is required to obtain more detailed and more accurate assessments of the hazards involved. With this need in mind, the Atmospheric Sciences Group at Lawrence Livermore Laboratory some months ago initiated work on a suite of research projects to improve understanding and assessment capabilities pertaining to the scavenging of debris from nuclear clouds. It is the intent of this paper to present an outline of each of these projects, their current status and some preliminary results.

The specific research problems to be discussed are as follows:

(1) A model of the interaction between a cumulus cloud and a nuclear debris cloud to determine possible enhancement or reduction in surface concentrations due to relative positions and motions. Among the assumptions used in the early calculations was that the vertical integral through cloud-center was deposited on the ground and integrated exposures and exposure rates were calculated based upon this deposition. It is possible, however, that debris will be entrained into a developing cumulus system and that the resultant vertical integral of the debris concentration in the cumulus cloud may be enhanced by this redistribution of radioactivity. Conversely, the resultant vertical integral may be decreased depending upon the relative vertical positions of the scavenging system and the debris cloud.

(2) A study of the microphysical interactions of debris particles with cloud droplets and raindrops to determine deposition rates. It is known that the rate at which the debris is removed from a cloud depends upon the rain rate, the spectrum of particle and raindrop sizes, the relative fall velocities of the raindrops and the particles, the efficiencies of capture for a given particle size, and the chemical properties of the particles. From these parameters washout and rainout efficiencies can be calculated and some measure of the effectiveness of the rainout process can be determined.

(3) A study to determine the feasibility of rendering the debris particles non-wettable. Particles resulting from free air bursts appear to be insoluble and wettable. This being the case, particles with radii as small as 0.1 μm can serve as condensation nuclei. According to arguments by Fletcher[3] and experimental results by Twomey,[4] particles whose surfaces depart from being completely wettable cannot serve as condensation nuclei under typical cloud supersaturations. Since nucleation scavenging appears to be the dominant rainout mechanism, a slight reduction in the particle wettability could greatly reduce the potential hazard from rainout.

(4) A study of the potential effects of dry deposition (deposition caused by the dispersion of debris particles to the surface) due to the detonation of a large number of low yield devices within a confined area.

(5) The development of a three-dimensional Atmospheric Diffusive Particle-in-Cell Code capable of

calculating the time-depending distribution of air pollutants under conditions of turbulent diffusion and wind shear.

A summary of the pertinent findings of the report Potential Exposures from Low-Yield Free Air Bursts[1] is included for the benefit of readers not familiar with this previous report.

Summary of the Pertinent Findings from Potential Exposures from Low-Yield Free Air Bursts

The risk due to fallout from a free air burst has generally been considered negligible since few particles large enough to settle to the ground are created. Early time rainout or washout of radioactive debris from air bursts has been considered a potential hazard[5] but since choice of meteorological conditions has always been available during testing, the probability of damage from this phenomenon has been considered small or non-existent. If, however, it becomes necessary to detonate many low yield devices within a small area, at a time when choice of meteorology is not an option, then hazards due to rainout or washout become much more probable.

Consider the following assumptions relating to the detonation of an all fission nuclear device:

1. It is detonated at a low altitude but high enough that there is no interaction of the fireball with the surface (free air burst).[5]
2. The resulting debris cloud rises to its stabilization altitude and is approximated in form by a right circular cylinder.
3. The distribution of radioactivity in the debris cloud at stabilization is assumed Gaussian in both the radial and vertical directions.
4. The debris cloud moves downstream at the speed of the wind at the stabilization altitude.
5. The debris cloud undergoes no shear.
6. The debris cloud is dispersed radially and vertically by diffusive eddies in the atmosphere.
7. At some point downstream, the debris in the debris cloud is subjected to scavenging by a rain bearing system, thereby causing all or a portion of the radioactivity to be deposited upon the ground. This deposition process is assumed to be instantaneous.
8. Once the radioactivity is deposited on the ground, it remains in place.

Assuming the above sequence of events occurs, it is possible to calculate a rate of exposure and an infinite exposure to a person standing at the deposition point once a means of determining the areal concentration of the radioactivity is specified.

For this study, the areal concentration is defined as the radioactivity removed from a column of unit cross sectional area through the center of the debris cloud (also often referred to here as the vertical integral*). Thus as the

*Depending upon use, the term vertical integral may refer to the radioactivity deposited, the dose rate due to this radioactivity, or the infinite dose due to this radioactivity, and, unless otherwise specified, it refers to cloud center.

debris cloud moves downstream, its vertical integral can be calculated as a function of time from the diffusion parameters, and the pertinent exposures and rates can then be calculated. The vehicle for calculating the vertical integral is the Large Cloud Diffusion Code 2BPUFF.[6]

Table 1 represents the input parameters to 2BPUFF for vertical integral calculations of debris clouds from one, ten, and one-hundred kt detonations. The cloud dimensions, height or rise,[7] and meteorology[8] are based upon mean conditions. Two diffusion conditions, atmospheric dissipation (ϵ) and vertical diffusivity (K_z), are assumed in order to obtain a reasonable range of values of the vertical integral as a function of time.[6,9,10] Figure 1 shows the vertical integrals (converted to time of arrival dose rates) in R/hr for the three yields, and Fig. 2 shows the infinite whole body exposures. The time-dependence has been converted to dependence on distance from ground zero in both figures. It is seen that extremely large exposures and rates can occur at distances even as far as 1000 to 2000 km for the 100 kt case. However, another important factor is that the debris clouds for the large-yield bursts will rise to greater heights and some or all of the debris will no longer be available for scavenging because no rain bearing systems will reach high enough. Thus, based upon an estimate of types of scavenging systems, it has been assumed in this report that 100% of the 1-kt debris, the lower 10% of the

Table 1. Input cloud parameters for exposure calculations.

Yield (kt)	Center height (m)	Thickness[a] (m)	Radius[a] (m)	Gross[b] fission (pCi)	^{131}I (pCi)	Wind speed (km/hr)	Atmospheric dissipation, ϵ (ergs/g-sec)		Vertical diffusivity (cm^2/sec)	
							Slow diffusion	Fast diffusion	Slow diffusion	Fast diffusion
1	2,640	1760	920	4.44×10^{20}	1.4×10^{17}	39.6	0.5	3	1000	10,000
10	7,000	3060	2400	4.44×10^{21}	1.4×10^{18}	70.2	1	5	1000	10,000
100	11,700	5340	6000	4.44×10^{22}	1.4×10^{19}	72.0	0.7	3.5	1000	10,000

[a]Corresponds to two standard deviations from cloud-center concentration.
[b]After H+1 hr.

Table 2. Potential surface exposure and downstream exposure rates.

Yield (kt)	Fraction deposited (%)	Distance downwind (km)	Infinite whole-body external gamma dose (rem)	External gamma exposure rate at time of arrival (R/hr)
1	100	10	25,000	25,000
		100	200-1200	35-100
		1000	0.3-1.0	<0.01
10	10	10	5000	7000
		100	1000-1500	150-200
		1000	1-4	0.015-0.05
100	1	10	800	1200
		100	300-350	45-55
		1000	1.5-5	0.02-0.06

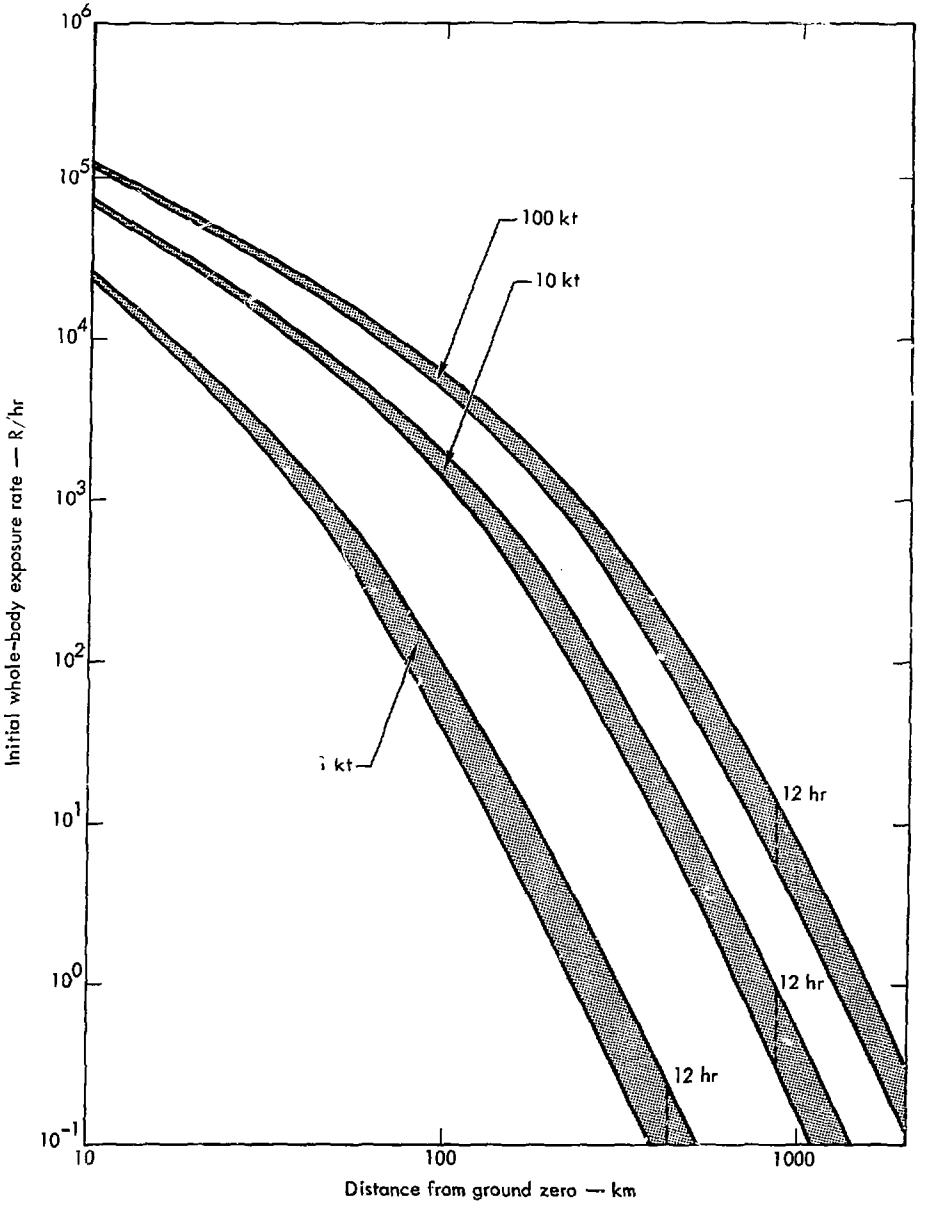

Fig. 1. Initial gamma exposure rate due to the deposition of the vertical integral at various distances from ground zero. The upper curve for each yield represents the case of slow horizontal diffusion; the lower curve represents the case of fast diffusion.

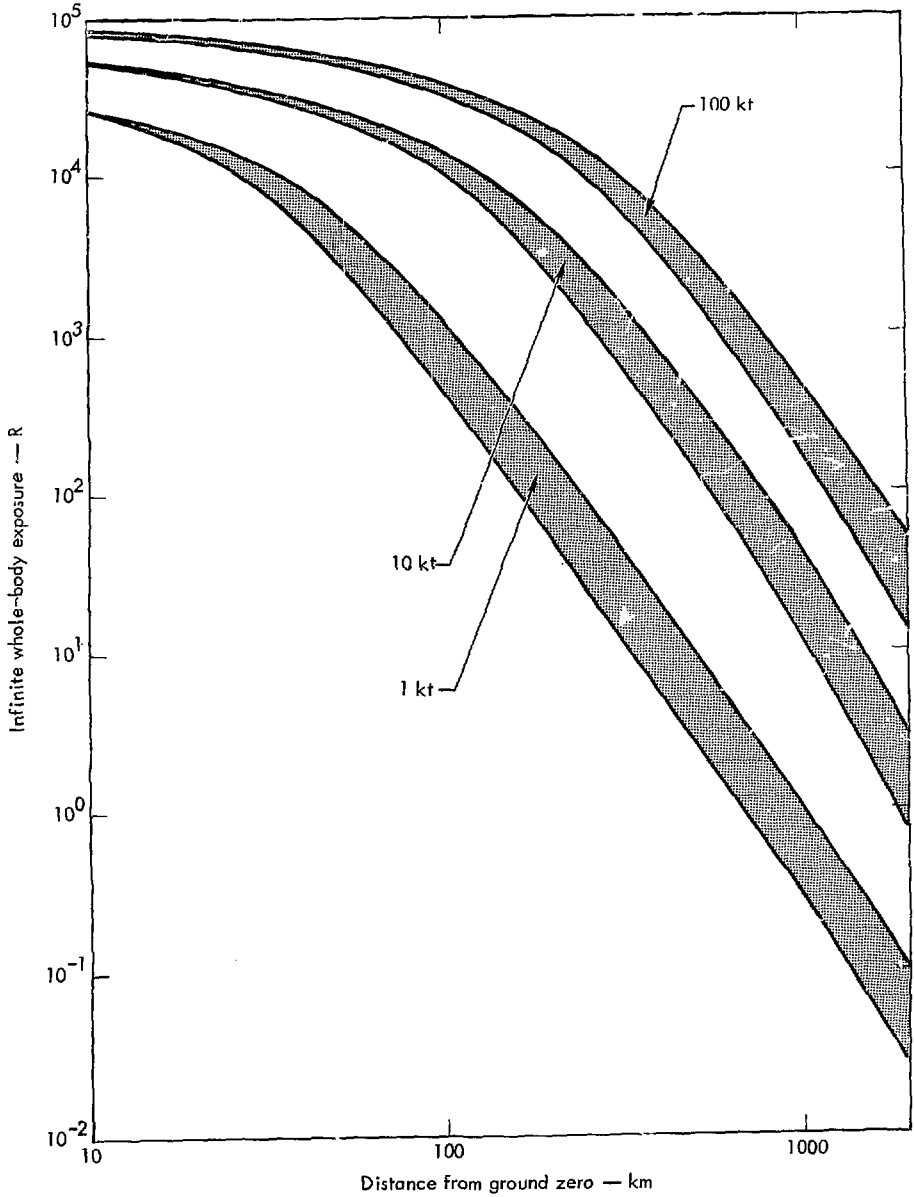

Fig. 2. Vertical integral (infinite whole-body exposure) due to gross gamma radiation as a function of distance from ground zero. The upper curve for each yield represents the case of slow horizontal diffusion; the lower curve represents the case of fast diffusion.

10-kt debris, and the lower 1% of the 100-kt debris are available for scavenging.

With these limits as a basis, Table 2 summarizes exposures and exposure rates for each of the three yields for distances of 10, 100, and 1000 km downstream from ground zero. Observe that while the total exposures due to the 10- and 100-kt clouds are reduced by factors of 10 and 100 respectively, rather high values can still occur even out to 100 km. It should be recalled, however, that the 10% and 1% availability of the 10- and 100-kt cloud debris was based upon a specific case and may be greater or less depending upon individual situations. For example, Conner and Phillips[2] in a similar calculation found that 100% of the radioactivity from the 10-kt cloud was available for scavenging based upon his calculations of stabilization height, cloud thickness, and height of scavenging systems.

Dynamic Effects of Convection

In the preceding section of this report it has been assumed that nearly all the debris in a vertical column from the ground up to the top of a rain cloud is scavenged by precipitation. But the presence of rain clouds implies the existence of dynamic effects which can greatly alter the vertical distribution of debris from that in the cloud-free environment.

Consider, for example, a simplified picture of the dynamics of a growing cumulus cloud. Moist unsaturated environmental air is drawn up through the base of the cloud and is accelerated upward because of buoyancy caused by the release of latent heat of vaporization. This indrawn air either remains a part of the young growing cloud or it leaves through the anvil top of a large fully developed cloud. The debris tends to move with the air so that the concentration of debris at all heights in a cumulus cloud developing in this manner would tend to be the same as the debris concentration of the environment in the vicinity of the base of the rain cloud. Now if the debris concentration is maximum near the rain cloud base, the amount of debris in a vertical column in the rain cloud will be much larger than the amount of debris in a corresponding column of the clear atmosphere. When rain falls, more than one times the vertical intergral of the debris concentration in the clear atmosphere can be brought to the ground beneath the debris-cloud center. In addition, the mass of air that passes through the rain cloud may be much larger than the mass of air in the cloud itself, further increasing the amount of debris that can be collected by drops and droplets and eventually brought to the ground. On the other hand, if the debris is primarily above the base of the rain cloud, it can be imagined that the cumulus cloud would grow up through the contaminated regions, pushing the debris aside and thereby preventing collection of debris by raindrops. From these simple examples it can be seen that the dynamics of individual convective cells are a major factor in controlling the amount of debris that enters the rain cloud and interacts with drops.

As debris moves through a rain cloud, some of the radioactivity is collected by raindrops and cloud droplets. Some of the cloud droplets are collected by falling raindrops while others evaporate when the cloud dissipates. The contaminated raindrops eventually fall to the ground, carrying with them all of the radioactive debris they have collected. Therefore, the debris in a rain cloud that is collected by raindrops is scavenged, and the radioactivity that does not get into raindrops is left in the atmosphere. Consequently the microphysical processes by which debris particles get into raindrops are the major factors that determine what fraction of the debris passing through a precipitating system is actually scavenged.

The remainder of this section is devoted to a description of a simple model of cumulus convection that has been used to estimate the typical range of values for the ratio of the vertical integral of the debris concentration inside a rain cloud to a similar vertical integral in the cloud-free environment. This ratio of vertical integrals is given the name enhancement factor, although enhancement factors less than 1 correspond to cases in which the rain cloud contains less debris than the environment. In following sections of this report, the scavengability of debris particles and the microphysical processes by which debris is collected and brought to the ground with falling raindrops will be discussed.

DESCRIPTION OF THE MODEL

A one-dimensional steady-state cumulus dynamics model has been used to estimate the importance of the dynamics of cumulus convection on the scavenging of debris from the atmosphere. This model was developed by Weinstein and Davis (1968).[11] It follows a sample parcel of air rising through a rain cloud; the cloud as a whole is assumed to be made up of many of these parcels one on top of the other and each with the properties of the sample parcel at the appropriate level; hence the structure of the rain cloud does not change with time. The sample parcel is initially at cloud base and has a small upward velocity. The surrounding environment has a vertical profile of temperature and moisture content determined from a standard radiosonde sounding. Calculations of the cloud temperature, vertical velocity, mixing ratio, cloud water content, hydrometeor water content, and updraft radius are made for the sample parcel at each level in the model cumulus cloud. The sample parcel also interacts with the surrounding environment by entrainment. The parameterized entrainment rate, μ, is taken from experimental studies of buoyant jets and bubbles and is given by the expression

$$\mu = \frac{1}{M}\frac{dM}{dz} = \frac{0.2}{R_c},$$

where M is the mass of air, z is height, and R_c is the radius of the core of the updraft. Further details of the dynamic and microphysical model are given in the above cited reference.

In addition to the rain cloud properties already mentioned, calculations of the concentration per unit mass of debris at each level in the cumulus cloud are included in the numerical model. The only process that alters the concentration of

debris within the sample parcel is entrainment of environmental air with a different debris concentration; therefore the concentration per unit mass of debris in the cloud at level ℓ, χ_ℓ, can be related to the concentration per unit mass of debris in the cloud at the previous lower level, $\chi_{\ell-1}$, by the expression,

$$\chi_\ell = \frac{\chi_{\ell-1} + \mu C_\ell \Delta z}{1 + \mu \Delta z},$$

where C_ℓ is the concentration per unit mass of debris in the environment outside the cloud at level ℓ, μ is the mass entrainment rate, and Δz is the thickness of the layer. At the lowest level of the model (at base of the cumulus cloud) the debris concentration is assumed to be equal to the environmental debris concentration. The numerical value of the entrainment rate, μ, depends on the updraft radius of the cloud which is, in turn, dependent upon the other physical properties of the rain cloud and the environmental sounding. Therefore, each cumulus cloud has a unique vertical distribution of debris just as each rain cloud has its own vertical distribution of drop concentrations, updraft radius, vertical velocity, etc. The question of whether debris is collected by drops or droplets is not considered in this simple model although it is of crucial importance when considering the scavenging of debris.

DESCRIPTION OF THE PRECIPITATING CLOUD

The radiosonde sounding for Salt Lake City on 16 May 1971 at 1200Z was used to describe the environment in which precipitating clouds developed. Scattered showers were occurring in the area at this time. The radar-measured tops of rain clouds were between 6000 m and 9000 m, and their bases were at 2700 m. The assumed updraft radius at cloud base was 1 km and the assumed updraft velocity at cloud base was 2 m sec^{-1}. The freezing temperature for all drops and droplets was assumed to be -25°C, a temperature which occurred at an altitude of about 6100 m. The thickness of the layers in the model was 200 m.

The environmental and in-cloud temperature profiles are displayed in Fig. 3. At low levels the in-cloud temperature is higher than the environmental temperature, primarily because of the release of latent heat as water vapor condenses. This positive buoyancy accelerates the parcel upwards as can be seen in the plot of vertical velocity in Fig. 4. The jog in the in-cloud temperature profile at 6100 m is due to the sudden freezing of all drops and droplets at this level and the resultant release of the latent heat of fusion. This positive buoyancy leads to a corresponding increase in vertical velocity at levels just above 6100 m and indicates the importance of freezing in the dynamics of cumulus convection. Above 7300 m the buoyancy of the parcel is negative and the vertical velocity drops to zero at 7900 m, which is, by definition, the top of the rain cloud. Two other factors also tend to decrease vertical velocity: the drag of drops and droplets which are carried along with the parcel, and entrainment of stationary environmental air. A cloud top of 7900 m is consistent with radar measurements of the heights of rain clouds in the Salt Lake

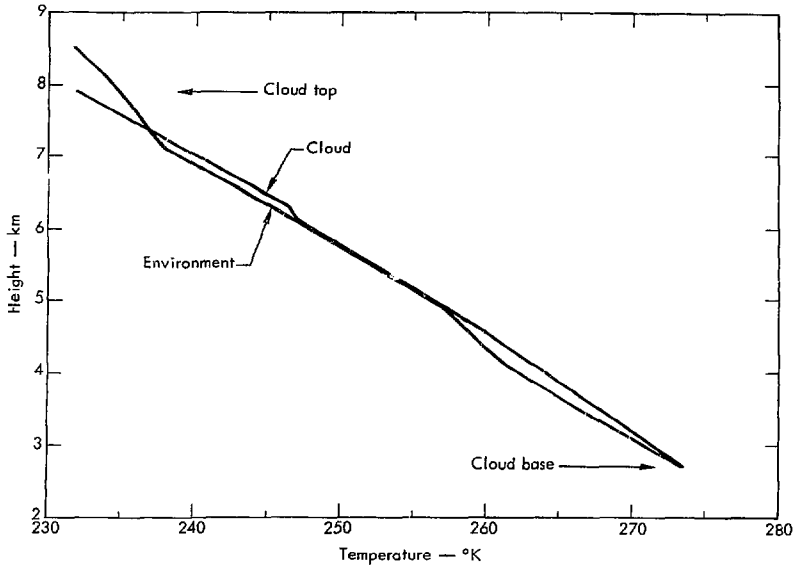

Fig. 3. Variation of temperature with height in the environment and in the model cloud.

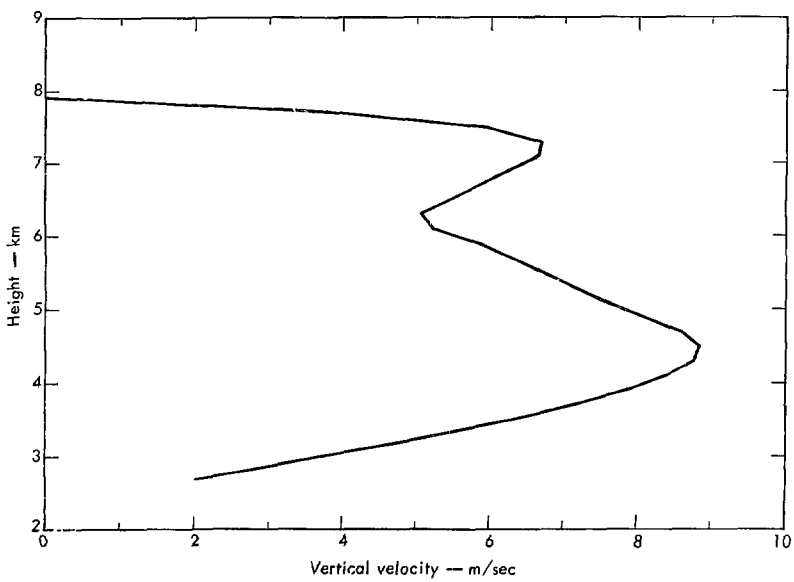

Fig. 4. Distribution of vertical velocity with height in the model cloud.

City area at the time of the radiosonde sounding.

The vertical distributions of cloud droplet mixing ratio and raindrop mixing ratio of hydrometeor water are shown in Fig. 5. Cloud droplets are formed by condensation of water vapor in the rain cloud and are removed by collection by hydrometeors. Raindrops are formed from cloud droplets and grow by coalescence. There is no mechanism in the model for a decrease of hydrometeor water in the sample parcel; therefore the raindrop water content must increase with height and be a maximum at the top of the cloud. In natural rain, fallout of drops would greatly alter this particular profile. The discontinuity in the slope of the cloud droplet concentration curve at 6100 m is due to the freezing of drops at that level, and to changes in certain microphysical parameters at the freezing level. If all the hydrometeor water in the rain cloud at any instant fell to the ground, there would be 1.6 mm of rainfall.

The characteristics of cumulus clouds that affect the vertical distribution of debris most directly are the updraft radius and the entrainment rate; these quantities are plotted in Fig. 6. The mixing rate is greatest in the region of smallest updraft radius which corresponds to the height of the largest updrafts. At levels where the vertical velocity is small the entrainment rate is also small. At the top of the rain cloud approximately two-thirds of the mass in the sample parcel is air that has been entrained by the rising parcel; the other one-third is air that entered at cloud base.

DEBRIS DISTRIBUTIONS

The environmental debris distribution that was used for the model calculations was taken from results of a 2BPUFF diffusion code (Crawford, 1966)[6] calculation. The debris concentration 100 km downwind from the detonation in the free atmosphere of a 1-kt all-fission device has a Gaussian profile with a peak concentration of 5×10^{-3} Ci/m^3. The height of this peak concentration is 2800 m and the standard deviation of the profile in the vertical is 500 m. It is assumed that the variations of concentration in the horizontal can be neglected over the region that interacts with the model cumulus cloud, and values at the center of the debris distribution in the horizontal are used.

The vertical profiles of debris concentration in the environment and in the rain cloud for a 1-kt free-air burst which interacts with the model cloud after moving downwind 100 km are shown in Fig. 7. Since the peak environmental debris concentration occurs at the base of the rain cloud, the debris concentration in the cloud is large. Mixing of cleaner environmental air as the parcel rises decreases the debris concentration in the cloud, but because entrainment is a relatively inefficient process the debris concentration remains high at all levels. Since the cumulus cloud model does nothing to alter the debris concentration below the rain cloud base, both profiles are identical below 2700 m. The enhancement factor, which has been defined as the ratio of the vertical integrals of the two profiles in Fig. 7, has a value of 3.04. This implies that if all the debris

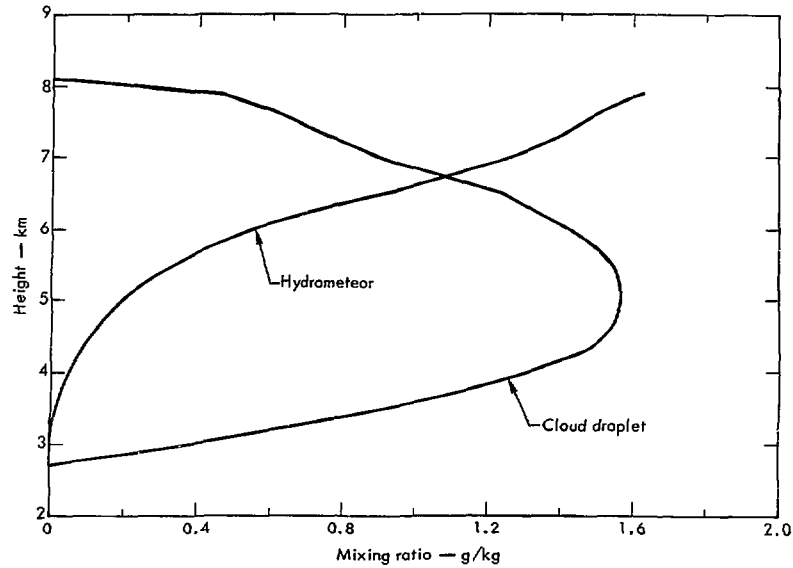

Fig. 5. Vertical distribution of liquid water components (cloud droplets and rain drops) in the model cloud.

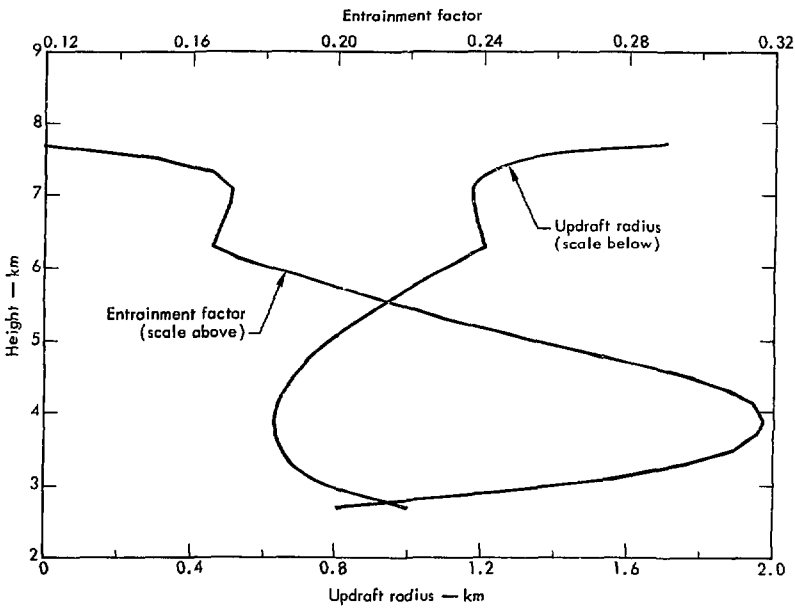

Fig. 6. Variation of entrainment factor and size of the updraft with height for the model cloud.

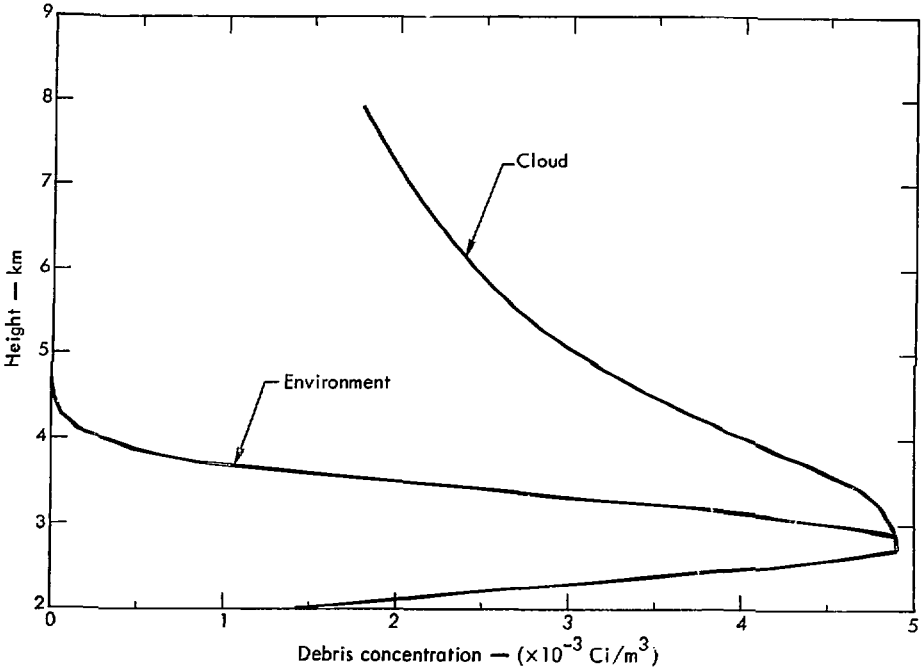

Fig. 7. Vertical distribution of debris in the environment and in the model cloud for a 1-kt all-fission free-air burst. The debris is assumed to interact with the rain cloud after moving downwind 100 km with the rain cloud where the height of the peak concentration for the Gaussian environmental profile is at 2.8 km and the standard deviation in the vertical is 0.5 km.

in and below this cumulus cloud were brought scavenged, approximately three times the vertical integral of debris in the environment outside the cumulus cloud would be brought to the ground with the rain.

It is apparent from the previous example that the debris concentration at the base of the rain cloud is a very important factor in controlling the debris concentration in the entire rain cloud. Therefore, additional sample calculations have been performed for several other environmental debris distributions interacting with the same cumulus cloud; the only change is in the height of the peak debris concentration. These results are illustrated in Figs. 8 through 12 and are summarized by the data in Table 3.

From the data it can be seen that the enhancement factor is largest when the maximum value of concentration occurs at the base of the rain cloud. When the peak concentration is below cloud base the enhancement factor is still greater than 1, except for the limiting case when all the debris is below cloud base, then the two profiles are identical and the enhancement factor is 1.0.

When the height of the peak environmental concentration is found at greater levels above the base of the rain cloud,

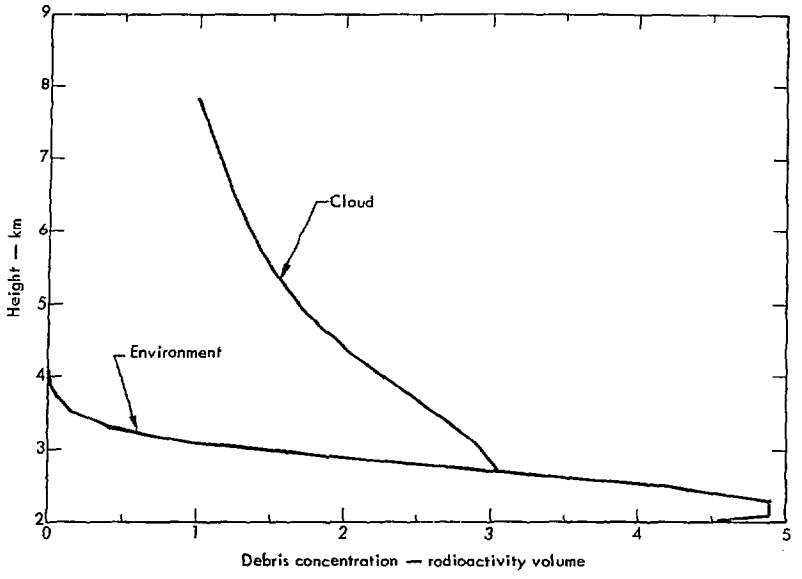

Fig. 8. Vertical distribution of debris in the environment and in the model cloud for a hypothetical free-air burst with the assumed height of the peak concentration of the Gaussian environmental profile at 2.2 km and the standard deviation in the vertical of 0.5 km. Numerical values for the ordinate would depend on the total amount of radioactivity released by the free-air burst.

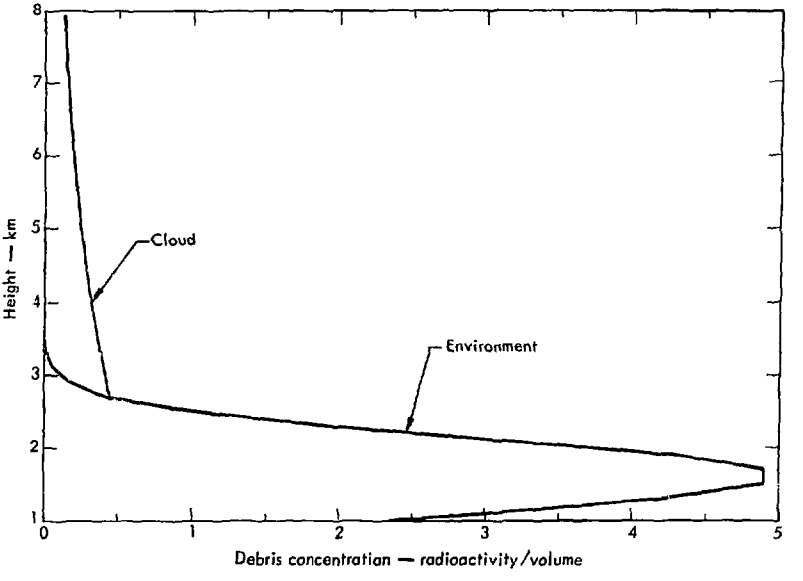

Fig. 9. Same as Fig. 8, except that the assumed height of the peak environmental concentration is 1.6 km.

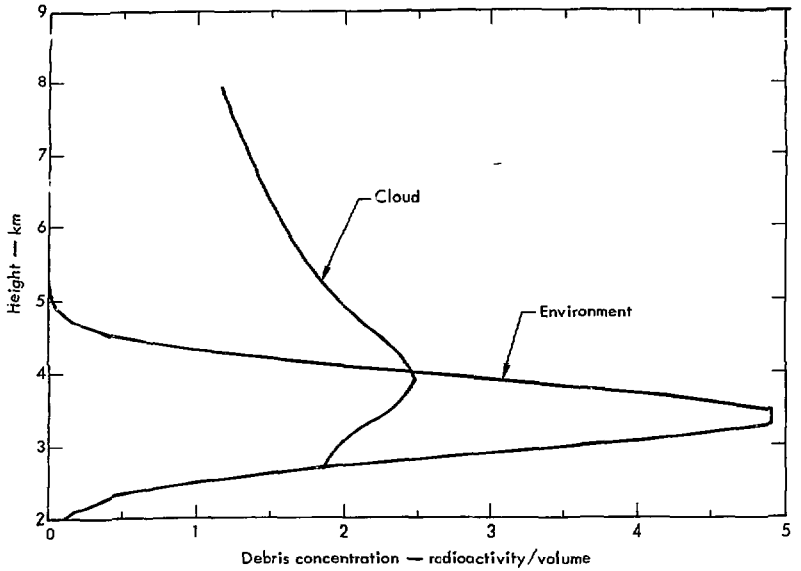

Fig. 10. Same as Fig. 8, except that the assumed height of the peak environmental concentration is 3.4 km.

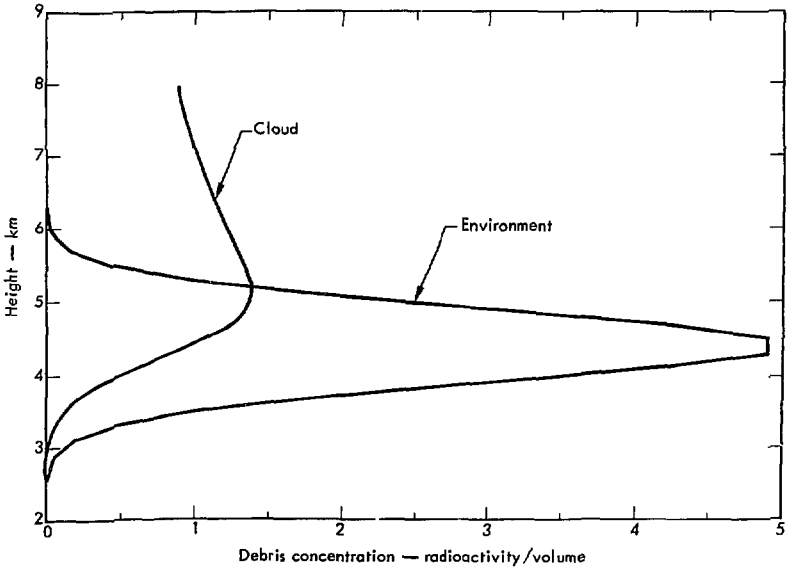

Fig. 11. Same as Fig. 8, except that the assumed height of the peak environmental concentration is 4.4 km.

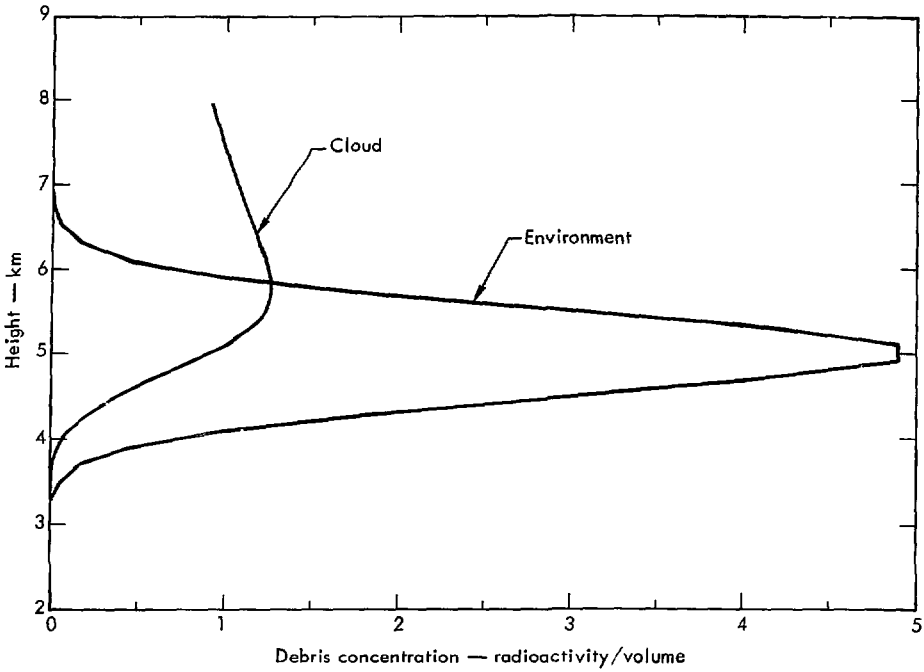

Fig. 12. Same as Fig. 8, except that the assumed height of the peak environmental concentration is 5.0 km.

Table 3. Important parameters for comparison of debris profiles.

Figure	Height of peak environmental concentration (m)	Standard deviation in the vertical of environmental concentration (m)	Concentration at cloud base ($\times 10^{-3}$ Ci m^{-3})	Enhancement factor
7	2800	500	4.90	3.04
8	2200	500	3.03	2.32
9	1600	500	0.44	1.20
10	3400	500	1.88	1.60
11	4400	500	0.02	0.73
12	5000	500	0	0.60
13	4100	1000	1.88	1.21
14	4500	1000	0.99	0.88

transport of debris into the cumulus cell by entrainment becomes more important, since only a small amount of debris enters through cloud base. At levels where the debris concentration in the environment is greater than the debris

concentration in the rain cloud, entrainment increases the debris concentration in the cloud. Conversely, at levels where the debris concentration in the environment is smaller than the debris concentration in the rain cloud, entrainment decreases the concentration of debris in the cloud. Consequently, the peak concentration in the precipitating cell occurs above its base and also above the height of the peak environmental concentration. Also, the concentration of debris in the rain cloud in lower regions is smaller than the concentration of debris in the environment, but at higher levels, once again, the precipitation region contains more debris. The value of the enhancement factor, which is maximum when the environmental debris concentration has its peak value at the base of the rain cloud, decreases as the height of the peak environmental concentration increases. The minimum value of the enhancement factor of 0 when the debris is completely above the rain cloud. The enhancement factor is greater than 1 only when significant amounts of debris enter the precipitating system through its base.

Additional representative calculations of debris profiles for the same model cumulus cloud are illustrated in Figs. 13 and 14; here the standard deviation of the environmental profile has been doubled. These results can be compared with two cases of the previous results, one for which the concentrations at the base of the

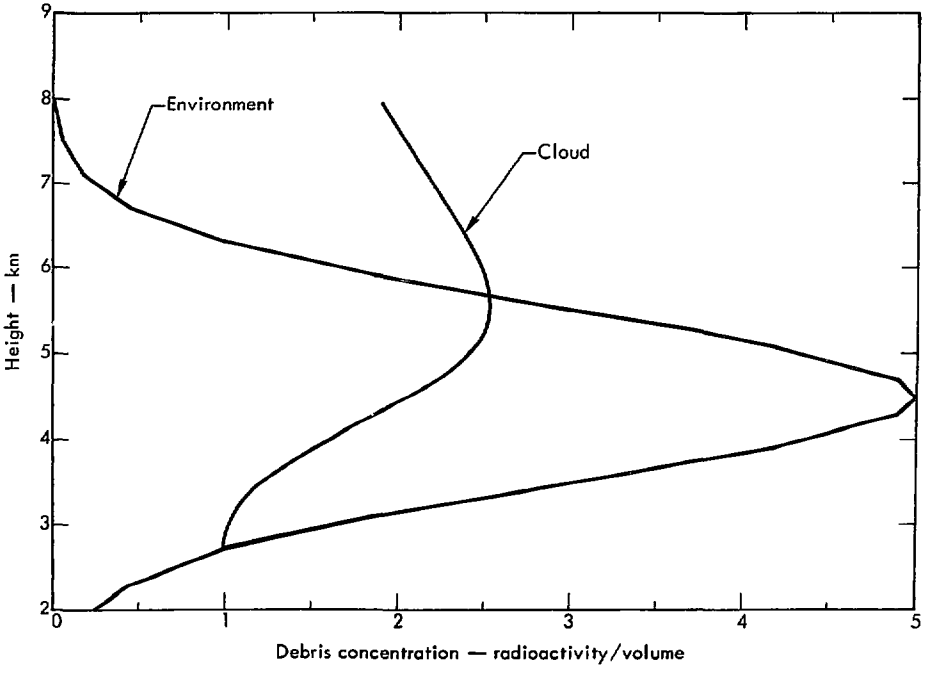

Fig. 13. Same as Fig. 8, except that the assumed height of the peak environmental profile is 4.5 km and the Gaussian standard deviation is 1.0 km.

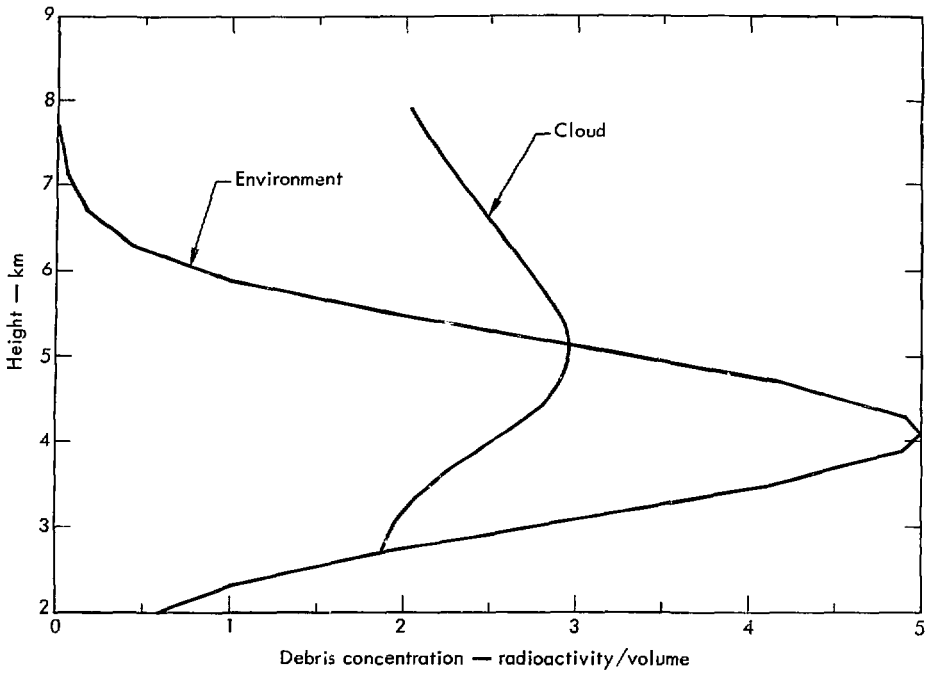

Fig. 14. Same as Fig. 8, except that the assumed height of the peak environmental profile is 4.1 km and the Gaussian standard deviation is 1.0 km.

rain cloud are the same (Figs. 10 and 13) in which case the enhancement factor is smaller for the broader profile, and the other for which the peak concentrations are at the same height (Figs. 11 and 14), in which case the enhancement factor is larger for the broader profile. This latter result follows primarily from the fact that the value of concentration at the base of the precipitation system is much larger for the broader environmental profile.

In summary, it has been shown that values for the enhancement factor will typically range from 0 to values of 3 or 4. The highest values occur when the base of a rain cloud forms near the level of peak concentration, in which case the amount of debris available for scavenging can be several times as large as the amount of debris that would have been present if the dynamics of convection had been ignored. When the debris is mostly above the base of the rain clouds the enhancement factor is less than 1 implying that the dynamics of convection tend to reduce the amount of debris that can be scavenged.

A Microphysical Description of Precipitation Scavenging

Aerosol particles are removed from the atmosphere by different processes depending on their size. Particles larger than about 1 μm can be scavenged by direct impaction with raindrops. This inertial capture process is the primary removal mechanism for washout or below-cloud scavenging, the washout efficiency being a function of particle size.

For rainout or in-cloud scavenging, other processes must be considered in addition to inertial capture. Aerosol particles with perfectly wettable surfaces and radii greater than 0.1 μm can serve as nucleation sites for the formation of cloud droplets. Soluble particles with radii as small as 0.01 μm can be nucleated in clouds. According to arguments by Fletcher[3] and experimental results by Twomey[4], an insoluble particle whose surface departs from being completely wettable, i.e., the contact angle is greater than say 6°, cannot serve as a condensation nucleus for typical cloud supersaturations. Nucleated particles can be deposited on the ground either through growth by diffusion to raindrop size and falling (a very rare event) or growing to several microns in radius and being accreted by a raindrop.

Particles of radius less than about 0.02 μm display considerable Brownian motion under atmospheric conditions, allowing them to collide and attach to droplets or raindrops. This scavenging mechanism is directly effective only for short times after the particles are formed since, given time, they will readily attach to larger debris particles or to natural aerosol particles. Those particles attached to droplets due to Brownian capture can be removed to the ground through accretion of the droplet.

Fallout particles from free air bursts consist mainly of oxides of the dominant casing materials. The various radionuclides make up a small percent of the total particle mass. Indications are that particles are insoluble in water and are wettable due to their large surface energy compared to that of water. Some of the radionuclides are soluble although it is not clear if the amount of soluble material on the particle surface can significantly change the nucleation characteristics as suggested by Hicks.[12]

Indications are that the particle size resulting from free air bursts are distributed log-normally and that the mean particle size decreases with increasing yield.[13,14] It appears reasonable to expect low yield air bursts to produce particles susceptible to inertial capture and nucleation scavenging. However, higher yields may produce particles below the nucleation threshold, leaving Brownian scavenging as the dominant removal mechanism.

In the remainder of this section an attempt is made to formulate the dominant scavenging processes discussed above. The model will be concerned with describing the removal of debris from a parcel of air in which the rain rate is constant throughout. It is further assumed that the concentration of debris particles, cloud droplets, and raindrops can be considered spatially uniform inside this parcel.

Each of the dominant removal mechanisms involve the collision and subsequent collection of a debris particle, or a water droplet which contains the particle, by a raindrop. Denoting as $n(r, t)\, dr$ the number of these target spheres of radius between r and $r + dr$ per unit volume of air at time t, the rate at which such spheres are removed by falling raindrops is:

$$\frac{\partial n(r, t)}{\partial t} = -\Lambda (r, t)\, n(r, t) \qquad (1)$$

$\Lambda(r, t)$ is the rate at which one target particle of radius r is removed from the volume at time t. A solution to this equation can formally be written as:

$$n(r, t) = n(r, o)\, \exp \left\{ -\int_o^t dt' \, \Lambda(r, t') \right\}, \qquad (2)$$

where

$n(r, o)$ is $n(r, t)$ evaluated at $t = 0$.

An expression for $\Lambda(r, t)$ as given by Chamberlain[15] can be written as:

$$\Lambda(r, t) = \int_o^\infty dR\, N(R, t)\, \pi R^2 [V(R) - v(r)] \times E(R, r, \xi). \qquad (3)$$

Here $N(R, t)$ is the number of raindrops per unit volume with radius R and fall velocity $V(R)$. $E(R, r, \xi)$ is the collision efficiency of the raindrop with a target sphere of radius r and mass density ξ. $v(r)$ is the fall velocity of the target sphere.

Scavenging by diffusiophoresis and thermophoresis does not appear to be important. The thermophoretic force on a submicronic particle juxtaposed with a droplet undergoing diffusional growth dominates the diffusiophoretic force[16] causing the particle to be repelled from the droplet. Although the attractive diffusiophoretic force dominates for particle sizes greater than about 1 μm, the resulting increase in the collision efficiency when the diffusiophoretic force is accounted for is of little significance.[17]

The removal rate given by Eq. (3) depends on time through the time dependence of the drop spectra. This expresses the fact that throughout the history of a cloud the number of drops of radius R in any unit volume changes with time. Under the assumption that the drop size distribution is time independent, Eq. (2) reduces to:

$$n(r, t) = n(r, o)\, \exp [-\Lambda(r) t]. \qquad (4)$$

For computation of the removal rate, $\Lambda(r)$, the terminal velocities of the drop given by LeClair, et al.[18] are used for Reynolds number less than 400 and for larger drops those of Gunn and Kinzer.[19] Terminal velocities of the collected sphere are assumed to obey Stoke's law and the collision efficiencies used are those of Langmuir.[20] The drop spectra is taken from results by Best[21] and can be written as,

$$N(R) = \frac{12 n\, W}{\pi\, a^n} (2R)^{n-4} \exp \left\{ -\left(\frac{2R}{a} \right)^n \right\} \left(\frac{1}{cm^4} \right). \qquad (5)$$

Here $n = 2.25$, W is the mixing ratio and a is a constant dependent upon rain rate. Values of W and a quoted by Best[21] for various rain rates, I, are given in Table 4. The drop spectrum is defined here such that $N(R)\, dR$ represents the number of drops per unit volume with radius between R and $R + dR$.

Debris particles of radius greater than about 1 μm are subject to inertial

Table 4. Values of a and W corresponding to different rain rates, I. From Ref. 21.

I $\frac{mm}{hr}$	a(cm)	$W \times 10^9$ $(cm/cm)^3$
0.5	0.1107	37
1.0	0.13	67
2.5	0.1608	145
5.0	0.1888	261
10.0	0.2218	470
25.0	0.2743	1020

capture by raindrops. Mathematically this situation can be described by Eqs. (1)-(4) where the collected particle is taken as a spherical debris particle. From Eq. (4) the fraction of debris particles of radius r which have been removed from the parcel at time t is:

$$F_1(r, t) = \frac{n(r, o) - n(r, t)}{n(r, o)}$$

$$= 1 - \exp[-\Lambda_1(r)t]. \qquad (6)$$

Assuming that every particle captured by a drop gets deposited on the ground, $F_1(r, t)$ gives the fraction of particles of radius r originally in the air that reach the ground as a function of time.

Considering inertial capture to be the only scavenging mechanism for washout, Eq. (6) gives the fraction of particles of radius r removed from a below-cloud parcel as a function of time. Figure 15 gives calculated values for the washout efficient, $\Lambda_1(r)$, as a function of particle size for various rain rates assuming a particle mass density of 5 g/cm^3. These values substantually agree with those found by Chamberlain.[15]

Values of the washout coefficient are sensitive to the size distribution of drops. Using values of the drop spectra found by Mason and Andrews[22] for warm frontal showers, the washout coefficients are about a factor of 2 smaller than those shown in Fig. 15. This indicates that the washout coefficient depends on type of rain shower as well as the rain rate.

In the present model, nucleation scavenging is calculated by assuming every debris particle of radius 0.1 m $\leq r \leq$ 10 μm serves as a condensation nucleus. The resulting droplet is assumed to immediately grow to 10 μm radius. Since the mass density of debris particles is typically greater than the density of water and of most natural aerosol particles, and further since there may be a significant number of debris particles with a radius of several microns, the density of the debris nucleated droplet is taken as:

$$\zeta = \left\{\zeta_p r^3 + \zeta_w \left(r_w^3 - r^3\right)\right\} / r_w^3. \qquad (7)$$

Here ζ_p is the density of the debris particle of radius r and ζ_w is the density of water. The radius of the nucleated droplet is r_w.

The fraction of debris particles of radius r removed from the parcel by nucleation and subsequent impaction with a raindrop is given in analogy with Eq. (5) and under the above assumptions as:

$$F_2(r, t) = 1 - \exp(-\Lambda_2(r)t). \qquad (8)$$

$\Lambda_2(r)$ is the removal rate for particles of radius 10 μm and density as shown in Eq. (7). Figure 16 represents the rainout coefficient, $\Lambda_2(r)$, for 0.1 μm $< r <$ 10 μm. For particles of radius greater than 10 μm, the rainout and washout coefficients are equal size since $\zeta = \zeta_p = 5$ g/cm^3. For

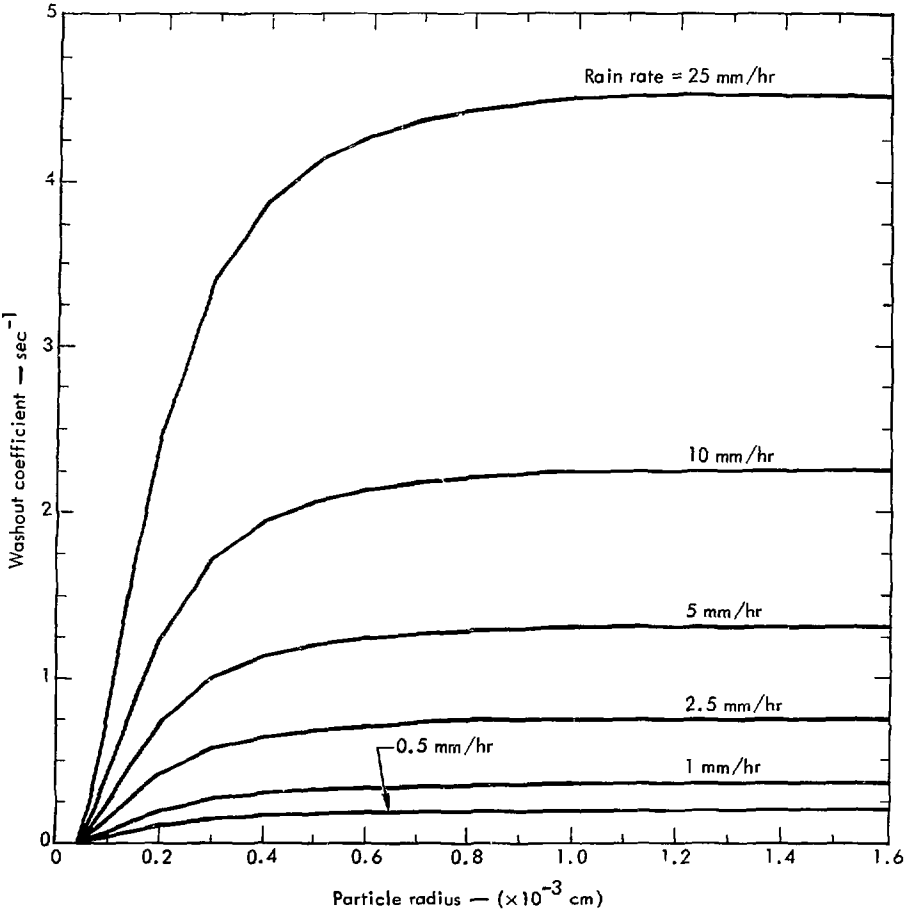

Fig. 15. Washout coefficient versus particle radius for various rain rates.

a given rain rate, Fig. 16 shows the rainout coefficient to be relatively constant for the particle sizes considered.

In order to make a complete rainout assessment, one should have details of the size distribution of debris particles. However, as a result of the assumption that every debris particle between 0.1 and 10 μm radius serves as a condensation nucleus when subjected to a cloud environment, a further simplification concerning the rainout calculation becomes apparent. Let m(r) dr represent the mass contained in debris particles of radius between r and r + dr. The total mass of debris deposited on the ground by particles of radius greater than 0.1 μm becomes:

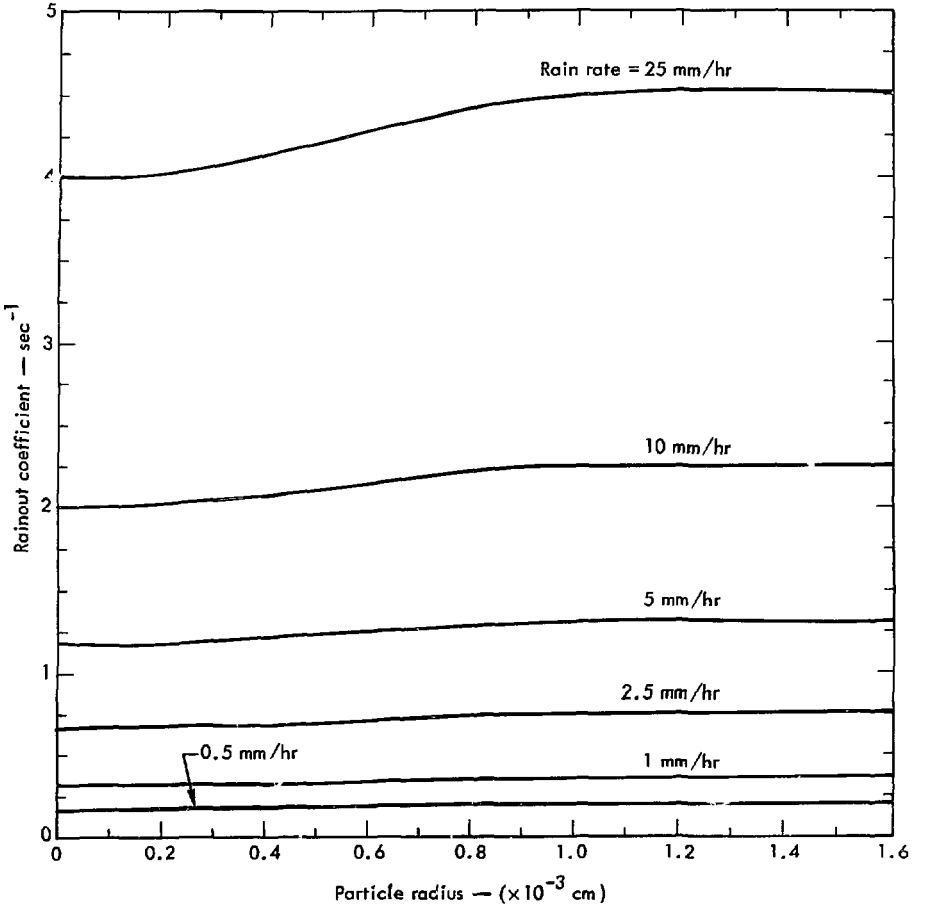

Fig. 16. Rainout coefficient versus particle radius for various rain rates.

$$M(t) = \int_{0.1\ \mu m}^{\infty} dr\ m(r) \times [1 - \exp(-\Lambda_2(r)t)]. \qquad (9)$$

$$M(t) = \left(1 - e^{-\Lambda_2^t}\right)\int_{0.1}^{\infty} dr\ m(r) = \left(1 - e^{-\Lambda_2^t}\right) M_o. \qquad (10)$$

Here Λ_2 is the rainout coefficient for a particular rain rate as plotted in Fig. 16. Since $\Lambda_2(r)$ is a weak function of r, Eq. (9) can be approximated by:

Here M_o is the mass contained in particles of radius greater than 0.1 μ. Under the further assumption that the radioactivity is contained in particles of greater than

0.1 μm radius, which is approximately true for yields as low as 1 kt, the fraction of radioactivity deposited on the ground as a function of time is plotted in Fig. 17.

An evaluation of the potential hazard due to rainout from a 1-kt free-air burst based on the above results can now be made. Consider the debris system to

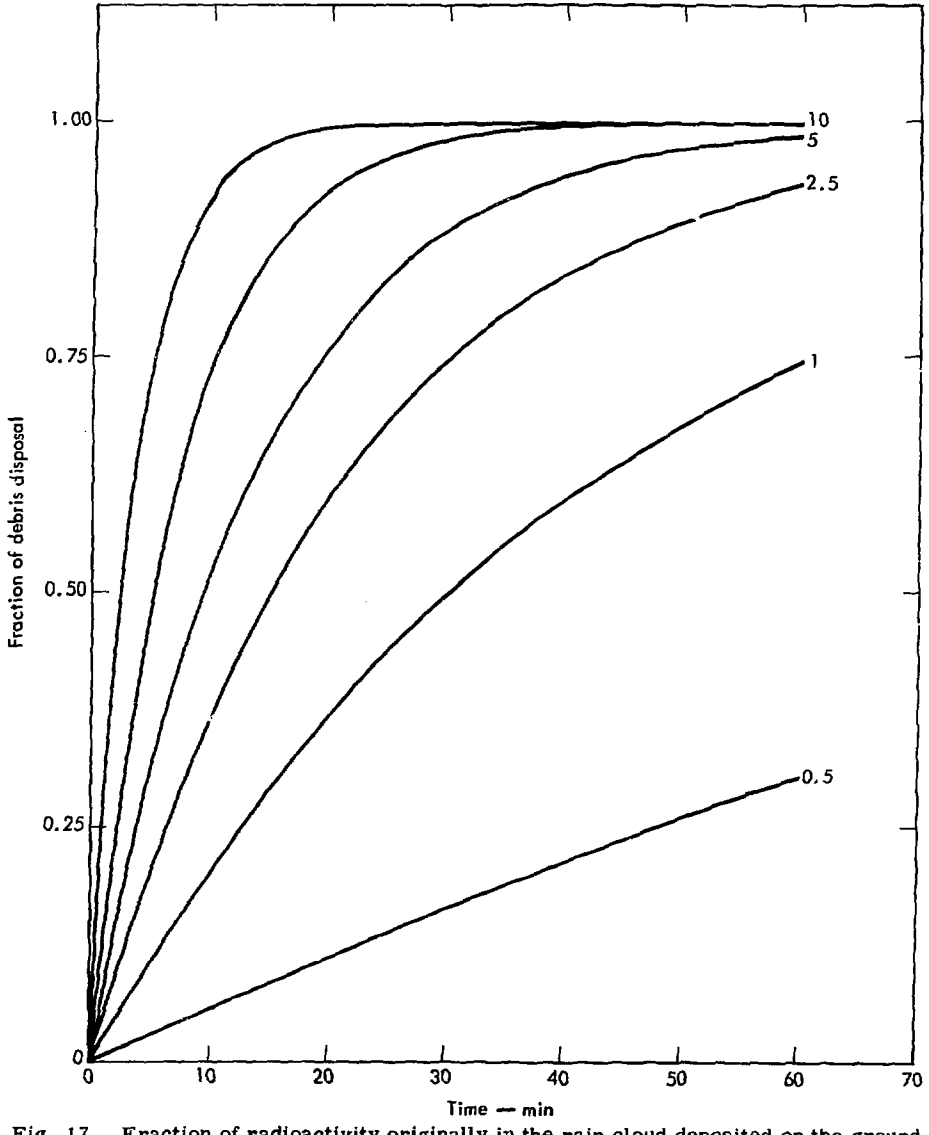

Fig. 17. Fraction of radioactivity originally in the rain cloud deposited on the ground versus time for various rain rates.

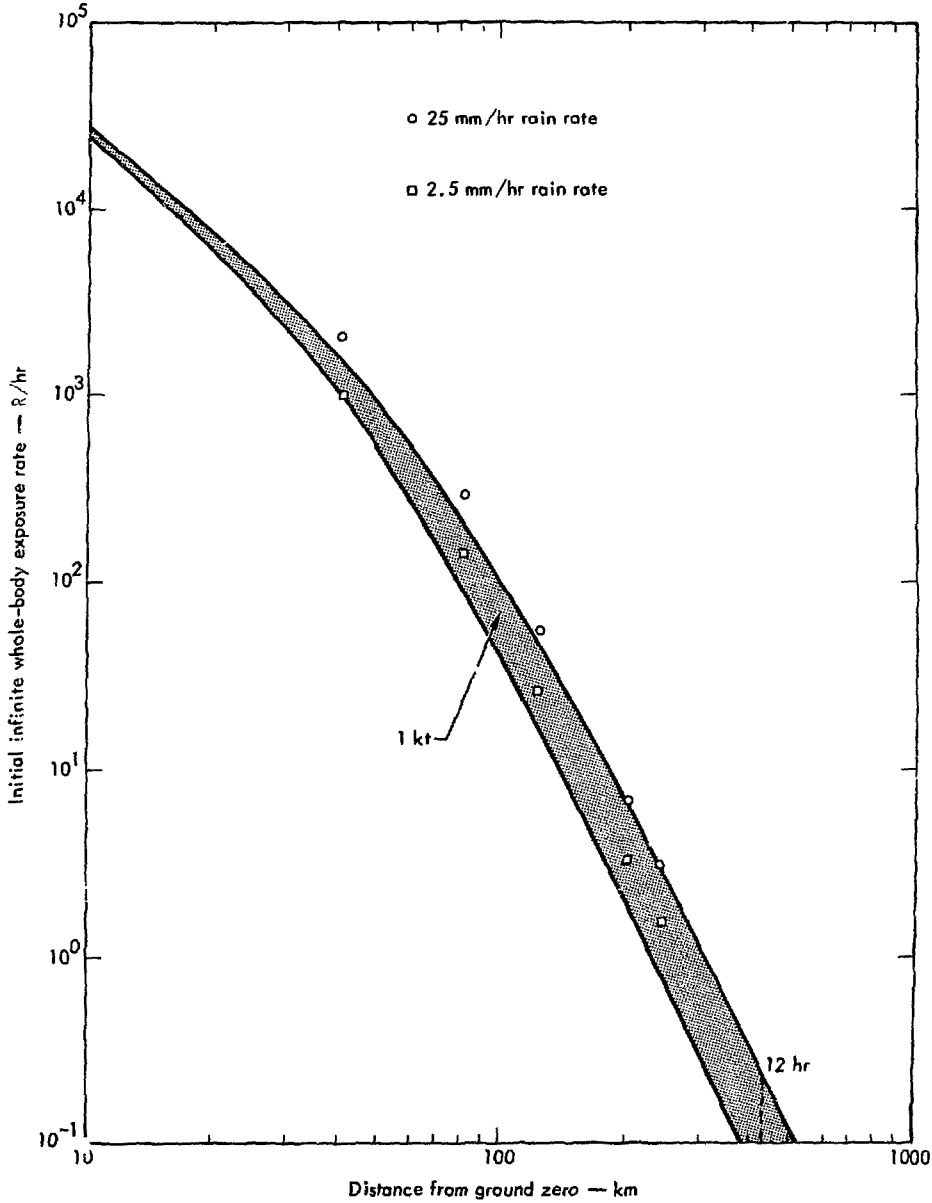

Fig. 18. Data points represent initial gamma exposure rates due to rainout of debris from a 1-kt free-air burst versus distance from ground zero. Rain is assumed to fall for 15 min with rain rates of 2.5 and 25 mm/hr. The solid curves are reproduced from Fig. 1.

move downwind and to diffuse according to the Lagrangian diffusion code (2BPUFF) under non-shear conditions with horizontal dissipation, ϵ = 1.8 ergs/g-sec. At various distances downwind the debris system is assumed to interact with a cumulus cloud, as described previously, giving an enhancement factor of 3. The radioactive particles are assumed uniformally distributed within the rain cloud and deposited by rainout as a function of time and for various rain rates as given in Fig. 17. Washout is neglected and it is assumed that the drops fall on the area directly below the rain cloud. The data points in Fig. 18 show values of the initial infinite whole body exposure rate versus distance downwind for rain rates of 25 and 2.5 mm/hr lasting for 15 min. The curves in Fig. 18 are reproduced from Fig. 1.

These new results on the potential hazards from rainout of debris from the 1-kt cloud are worthy of special comment, namely, that the results of the present analysis indicate that the potential dose as a function of range for rainout (Fig. 18) constitutes a reasonable estimate of the expected hazard for the conditions cited. This expected estimate level of hazard is quite comparable to that previously reported in "Potential Exposures from Low-Yield Free Air Bursts."[1] During the remainder of this contract year, the LLL Rainout Team will continue to refine the present estimate, as represented in Fig. 18, for effects of wind shear (not expected to be large in summer), and other assumptions inherent in the analysis. Further work is required in regard to the variation of particle size distribution with yield in order to extend the present analysis techniques to yields other than 1 kt. This work will be a portion of our proposal for the coming year. In the future we will also evaluate the probability associated with meteorological conditions consistent with Fig. 18 and other scenarios of interest to DNA.

Rainout estimates assuming nucleation scavenging and inertial capture were possible for a 1-kt free-air burst because in this case it appears that very few of the debris particles are smaller than 0.1 μm radius.[23] It appears that the mean particle size decreases with increased yield such that for higher yields a significant portion of the radioactivity is contained in particles smaller than 0.1 μm. This being the case, different scavenging mechanisms (probably Brownian capture) become important and the above analysis does not apply.

Thoughts on Altering the Scavenging of Debris Particles

The problem here is to change or to control the rate of rainout from clouds. We are studying the possibilities of changing their macrophysical dynamics by interfering with their microphysical processes. One can add to a cloud or take parts of it away, and at first look it appears that adding something is the easier operation.

There are a number of possible effects of additives on the microphysical processes of water and ice particle formation in a cloud that can influence the overall macrophysical dynamics of the cloud. Additives in the form of an excess number of nucleating agents could hinder the development of water and/or ice particles to a size large enough to precipitate out

of a cloud. Small amounts, a monolayer or even a partial monolayer, of materials with low surface energies adsorbed on to the high energy surfaces of nucleating particles can change their wetting characteristics and thus their nucleating rates and possibly put them into the nonnucleating category as far as the cloud is concerned. Small amounts of materials can also affect the electrical properties of the water and/or ice particles, the elastic and inelastic collision processes, the accommodation and reflection coefficients for the water molecule on water and ice, and change the condensation and/or evaporation rates of water molecules between water droplets and between water and ice particles.

Let us look at the use of additives to modify the rate of nucleation of particles by changing their wetting characteristics. We shall assume the validity of the Fletcher analysis[3] of heterogeneous nucleation of water vapor by insoluble particles as a function of particle size, contact angle and saturation ratio in the cloud. Figure 19 is a set of Fletcher's curves for a given nucleation rate. Since the saturation ratio in most clouds is about 1.001 and only under unusual circumstances may reach as high as 1.01, it can be seen from Fig. 19 that a particle with radius less than 10^{-6} cm will not act as a nucleation center. Even particles with a radius greater than 10^{-5} cm need to be almost completely wettable before they can act as nucleation centers for water vapor in a typical cloud.

The solid particles that are expected to be picked up or injected into a cloud would be metal oxides in the form of crystals or glasses and possibly some free metallic particles. All such particles have a large surface energy compared to water (73 ergs/cm^2). See Tables 5 and 6. One would expect water to wet and spread on all such particles,[29-31] and from the Fletcher analysis all such particles would be active nucleating agents in a cloud if they were 10^{-5} cm in radius or larger.[3]

The rates of nucleation by these solid high surface energy particles can be changed by the addition of low surface energy materials that will adsorb onto the surface of these particles in the cloud and lower their surface energies to less than that of water. A monolayer of

Table 5. Surface energies of various materials, taken from references cited.

Materials	γ at 0°K (erg/cm^2)	Reference
Oxides of General Formula MO		
MgO	1090	24
FeO	1060	24
MnO	1010	24
CaO	820	24
SrO	700	24
BaO	604	24
BeO	>1420	24
CdO	530	24
LnO	600	24
PbO	250	24
General Formula M_2O_3		
B_2O_3	79.5 @ 900°C	25
Al_2O_3	905 @ 1850°C	26
General Formula MO_2		
UO_2	642 ± 20%	24
ZrO_2	800 ± 20%	24
ThO_2	530 ± 20%	24
SiO_2	>800	24
TiO_2	>800	24

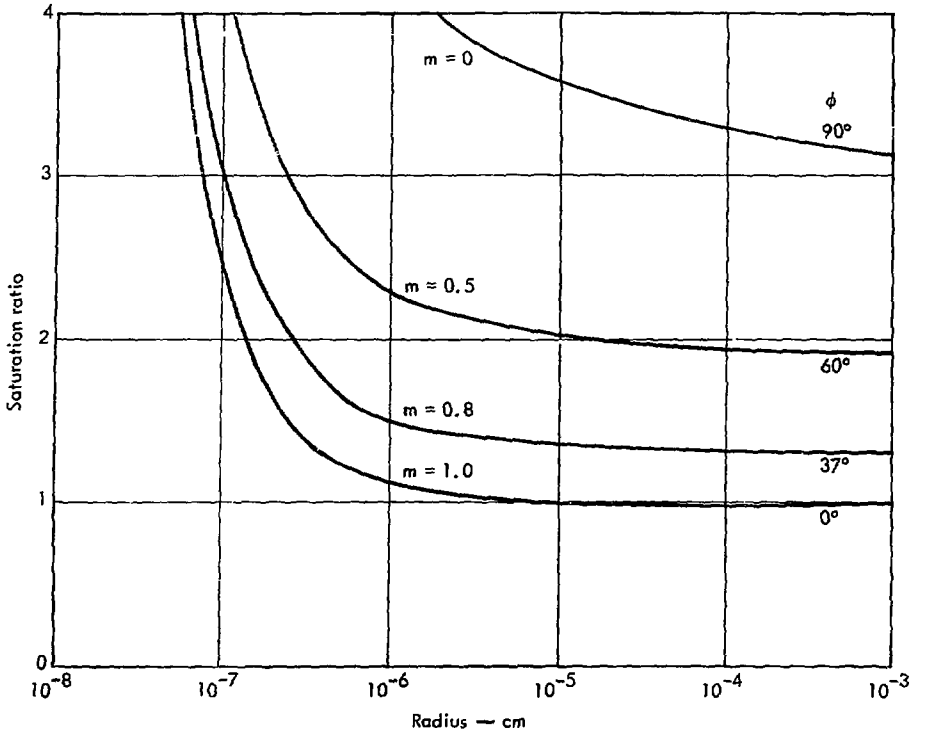

Fig. 19. Critical supersaturation ratio for nucleation of a water droplet in 1 sec on a particle of given radius and surface properties defined by m = cos ϕ where ϕ is the contact angle (from Ref. 3).

perfluoro fatty acid on platinum reduces its specific surface free energy from about 2000 ergs/cm^2 to about 10 ergs/cm^2.[32,33] The water should not wet nor spread on these particles. Even a small departure from perfect wettability will hinder the nucleation dynamics. There are a number of possible materials that could be selected, and these could be introduced into the cloud by rockets, balloons, smudge fires, antiaircraft guns, the device, etc. If one could make the additive available to be adsorbed onto the particles not much material would be needed. From Table 7 it can be seen that for each cm^3 of metal or metal oxide, subdivided into 10^{15} particles with sides of 10^{-5} cm, it would take only 10^{-5} mole of adsorbable material to give all particles a monomolecular coat.

For optimum control of rainout one may want to use one or more types of additives at the same time. It may be best to keep the insoluble particles from wetting by an adsorbable additive and to overnucleate the cloud with NaCl particles with masses equal to or greater than 10^{-2} grams per particle. This would

keep the insoluble particles from nucleating and furnish enough water soluble particles for nucleating centers to keep the droplets of water and particles of ice small enough so that they will not precipitate out and carry out the solid particles by impact.

Table 6. Surface energy of some metallic elements (at their melting points).[27,28]

Metal	Melting point (°C)	Surface energy, γ (ergs/cm^2)
Aluminum	660	900
Antimony	630	370
Beryllium	1400	1000
Cadmium	321	620
Cobalt	1495	1530
Copper	1083	1100
Gold	1063	1120
Iron	1534	1500
Lead	325	450
Magnesium	650	560
Mercury	-39	460
Nickel	1453	1700
Platinum	1769	1800
Silver	961	920
Tin	232	570
Tungsten	3410	2300
Uranium		
Zinc	420	790

There are a number of possible effects of additives on cloud dynamics about which little or nothing is known. Research into these effects is desperately needed.

It should also be kept in mind that a cloud is a dynamic system, and the applicability of equilibrium arguments is somewhat limited and may at times be misleading. The Knudsen equation, for instance, gives too large a gas transport to and from a water drop under nonequilibrium conditions. It is probable that the condensation and evaporation coefficients of water molecules at liquid water surfaces can be modified by as much as a factor of 10 by contaminating the water surfaces[34-36] or even aging them. There are many different combinations of factors involved in the interaction between incident water molecules and surfaces of water drops and ice particles. These factors are the:

Table 7. Surface area of a 1-cm cube with subdivision.

Length of side (cm)	Number of cubes	Total surface area (cm^2)	Moles of material to cover surface[a]
10^0	10^0	6×10^0	10^{-10}
10^{-1}	10^3	6×10^1	10^{-9}
10^{-2}	10^6	6×10^2	10^{-8}
10^{-3}	10^9	6×10^3	10^{-7}
10^{-4} (= 1 μm)	10^{12}	6×10^4	10^{-6}
10^{-5}	10^{15}	6×10^5	10^{-5}
10^{-6}	10^{18}	6×10^6	10^{-4}
10^{-7}	10^{21}	6×10^7	10^{-3}
10^{-8} (= 1 Å)			

[a]We assume that it takes 10^{13} molecules to cover each cm^2 and each mole has 6×10^{23} molecules.

- specific condensation coefficient,
- specific evaporation coefficient,
- thermal accommodation coefficient,
- momentum accommodation coefficient,
- extent of compliance with the cosine law for diffuse reflection, and
- extent the cosine law would obtain due to scattering from surface irregularities alone.

Even though Young[37] gave a correct form of the interaction of a liquid at equilibrium on a solid surface in 1805 it was only in 1959 that Johnson[38] gave a clear statement of the problem and a thermodynamic justification of Young's equation along the lines of Gibbs' derivation. The notion of a wetting tension was given by Dupré (1869),[39] and Cooper and Nuttall (1915)[40] gave the conditions for spreading and nonspreading. Harkins (1920-1941)[41] further developed the notion of a spreading tension more from the point of view of a gradient of the free energy of the system with respect to the area. All of the above developments are for equilibrium conditions and assume no electrification of the system. The molecular and/or atomic interaction mechanisms of wetting and wetting rates are not well understood. If one considers small drops on surfaces, ignoring inertial effects, one might expect the wetting rate of a surface to be expressed by equating the rate of change of the reversible work due to "capillary" forces to the rate of energy dissipation due to the viscous flow of the film over the surface. There are a number of efforts needed to understand the off-equilibrium dynamics in the microphysics of clouds.

Dry Deposition

One method by which radioactivity from air burst debris clouds may be deposited upon the ground, generally over long periods of time, is through the process of dry deposition. In this process the very small particles in the clouds are dispersed downward through the atmosphere by diffusive eddies. As the small particles reach the ground, they become attached to various surfaces which they may encounter and, unless removed, become sources of radioactivity at these points. The amount deposited upon a given surface depends upon a so-called velocity of deposition (or deposition velocity) defined[15] as

$$V_d = \frac{\text{Amount deposited per cm}^2 \text{ of surface per sec}}{\text{Volumetric concentration per cm}^3 \text{ above surface}}$$

where the volumetric concentration is measured very near the surface. Values of V_d vary from 0.1 to 10 cm/sec with most reported values near 1 cm/sec (see Ref. 15). Thus, to determine the total deposition, D, one needs a time history of the volumetric concentration χ near the surface in order to evaluate the integral

$$D = \int_{t_1}^{t_2} \chi \, V_d dt.$$

Of course decay must be accounted for when considering radioactive materials.

When the debris cloud from a free-air burst becomes stabilized and moves downstream, the concentration of radioactivity near the ground will usually be small

(depending upon height of stabilization) until the radioactive particles are dispersed downward by the action of vertical diffusion. Since this process can be expected to take some time and the amounts deposited are small for low concentrations, the potential threat from one or even a few bursts is seen to be quite small in most cases. An exception would be when the surface rises rapidly toward the higher concentrations near cloud center as in a range of mountains or high hills. If, however, a large number of low-yield bursts were detonated within a limited area, the resulting cloud would be large in horizontal extent but would be stabilized at a low altitude. The radioactive particles would soon become dispersed to the surface, and, due to the large horizontal size of the cloud, high surface concentrations could be present at a given point for long periods depending upon the time of passage of the cloud. Also, as the cloud aged and became very large horizontally, even a small surface concentration, when integrated over a long period of time may result in large values of dry deposition; this effect would be further enhanced at points far downstream if conditions were such that no or very little deposition of radioactivity occurred earlier.

The effect of wind velocity, i.e., the mean speed at which the debris cloud is carried downstream, will also have a bearing upon the total deposition since, for a given distance from ground zero, the mean speed will determine the amount of decay, and to some extent, the amount of dispersion of the radioactivity within the cloud.

Table 8 presents some calculations which demonstrate the effects of stabilization height and wind speed upon the infinite dose from gross gamma due to dry deposition over flat ground at various distances downstream from ground zero. It is assumed that the clouds are created by the detonation of 10 Mt of low yield devices within an area bounded by a radius of 80 km. The calculations were made using the computer code 2BPUFF[6] programmed with a deposition velocity of 1 cm/sec. Trials 1 through 3 demonstrate the relatively small exposures obtained from debris clouds which stabilize at heights of 5 to 6 km. The higher values in Trial 2 are caused

Table 8. Effects of stabilization height and wind speed on the infinite gross gamma dose due to dry deposition.

Trial No.	Cloud center height (km)	Wind speed (m/sec)	Initial thickness (km)	Dry deposition, R		
				200 km	2000 km	20,000 km
1	6	20	4.4	neg.	neg.	0.003
2	5	20	4.4	0.002	0.8	0.2
3	5	10	4.4	0.01	0.005	0.01
4	2	20	4.4	40	2	0.15
5	1	10	4.4	100	2	0.15
6	3	10	3.0	neg.	neg.	10

by experimental use of higher values of the vertical diffusivity. In Trial 4, the cloud center is lowered to 2 km and the thickness* is such that a reasonably high concentration is present at the surface at the time of stabilization. The circumstances are sufficient to cause large exposures close-in with decreasing but high exposures farther downstream. When the cloud center is lowered to 1 km (Trial 5), exposures are higher at all distances considered even though the windspeed is halved and the travel time therefore doubled with respect to Trial 4. Trial 6 was made to demonstrate the effect of a debris cloud in which diffusion and deposition are inhibited until the cloud is 20,000 km downstream, at which time a large vertical diffusivity is allowed to bring debris to the surface. This situation might represent the cloud's passage over a large cold dome of air and/or passing over an area in which a low-level temperature inversion is present for a long period of time. Furthermore, the increase at 20,000 km is partly due to the fact that the terrain was programmed to slope upward toward, but not to reach, cloud center, thereby simulating the effect of a debris cloud moving over a range of high hills or low mountains.

More work needs to be done on the effects of dry deposition. Deposition velocities over different surfaces and velocities of different particle sizes need to be considered, and the inhibitory effects of inversions and the enhancement effect of strong convection and overturning, as well as the extent to which sloping land increases or decreases deposition should be studied.

A Three-Dimensional Atmospheric Diffusion Particle-In-Cell Code (ADPIC)

ADPIC is a numerical three-dimensional Cartesian particle diffusion code, capable of calculating the time dependent distribution of air pollutants under many conditions, which include strongly distorted advection wind fields and calm conditions for which Gaussian models are not suitable. Basically the code solves the three-dimensional advection-diffusion equation in its conservative form (pseudo-velocity technique), for a given mass-consistent advection field, by finite difference approximations in Cartesian coordinates. The method is based on the particle-in-cell technique[42-44] with the pollutant concentration represented statistically by imbedded Lagrangian marker particles in an Eulerian grid. The inclusion of sources, sinks and gravity terms is planned. The capability of the grid to automatically expand and travel with a pollutant cloud, makes the code particularly suitable for the study of single puff releases, such as a free-air burst.

*The thickness of a debris cloud in which the debris is normally distributed in the vertical, as is the case here, is the distance between the two standard deviation concentration points; i.e., thickness = $4\sigma_z$.

THE METHOD

The pseudo-velocity method consists of the following: Given the nonlinear

transport-diffusion equation,

$$\frac{\partial Q}{\partial t} + \bar{U} \cdot \nabla Q = \nabla \cdot (K \nabla Q) \qquad (11)$$

where Q is a scalar concentration, K the diffusion coefficient and $\bar{U}$ the (given) mass consistent wind advection field, we can, under the assumption of incompressibility, replace the $\bar{U} \cdot \nabla Q$ term by $\nabla \cdot (Q\bar{U})$. Upon combining the two divergence terms we can rewrite Eq. (11) in its conservative (pseudo-velocity) form,

$$\frac{\partial Q}{\partial t} + \bar{\nabla} \cdot \left[Q\left(U - \frac{K}{Q}\bar{\nabla}Q\right)\right] = \frac{\partial Q}{\partial t} + \bar{\nabla} \cdot (Q\bar{U}') = 0 \qquad (12)$$

where $\bar{U}' = \bar{U} - K/Q\ \bar{\nabla}Q$ is the pseudo transport velocity.

The grid mesh of the code is represented by an Eulerian grid consisting of three-dimensional rectangular cells of uniform size. The concentrations Q are defined at the centers of the cells and the velocities $\bar{U}$, $\bar{U}'$ and $-K/Q\ \bar{\nabla}Q$ are defined at the cell corners. The locations of the particles, which represent the pollutant cloud statistically, are defined by their individual Lagrangian coordinates within the Eulerian fixed grid.

A time cycle of the code is divided into an Eulerian step and a Lagrangian step and proceeds as follows:

1. Eulerian Step: The concentrations, Q, given for each cell at the beginning of the cycle, are used to calculate the diffusivity velocities $\bar{U}_D = -K/Q\ \bar{\nabla}Q$ which are then added to the given wind advection velocities $\bar{U}$ to yield a pseudo velocity $\bar{U}'$ for each cell corner.
2. Lagrangian Step: Each marker particle contained in a given cell is transported for one time step Δt with a velocity $\bar{U}'_p$, which is computed from the pseudo velocities $\bar{U}'$ at the corners of the cell, and the particle coordinates $\bar{X}$ by a volume weighting scheme,

$$\bar{X}\ (\text{new}) = \bar{X}\ (\text{old}) + \bar{U}'_p\ \Delta t. \qquad (13)$$

3. Finally, a new concentration distribution, Q, is calculated from the new particle positions, which ends the cycle.

The chief advantage of using such a hybrid Eulerian-Lagrangian scheme is that the fictitious diffusion inherent in a purely Eulerian scheme is eliminated. The truncation errors inherent in the finite difference algorithms remain, of course, and must be minimized by the choice of the time-step.

The boundary conditions are implemented in a layer of boundary cells that surround the grid. In the case of a growing puff cloud the Eulerian grid will be expanded automatically, once a particle has moved into any of the boundary cells. Topography and inversion layer boundaries are represented by a deposition and reflection boundary conditions, respectively. The use of relative coordinates allows the grid to follow a pollutant cloud along its trajectory. The computer time required for a $15 \times 15 \times 15 = 3375$ cell Eulerian grid with 4000 particles is approximately one second per time cycle on a CDC 7600.*

*Reference to a company or product name does not imply approval or recommendation of the product by the University of California or the U.S. Atomic Energy Commission to the exclusion of others that may be suitable.

Future Work

Future plans include continued research into the areas outlined in this report. To account for shear effects on the debris system, a three-dimensional particle in cell diffusion code capable of calculating the time dependent distribution of debris under distorted advection wind fields is being developed and validated.

The dynamics of interaction between a debris system and a precipitating system determine the amount of debris available for scavenging and the time history of the wet deposition on the earth's surface. Future plans include adapting existing one- and two-dimensional time-dependent rain cloud models to describe the interaction of a precipitating system with a debris cloud. Incorporation of a microphysical description of scavenging into these numerical rain cloud models will enable estimates to be made of the fate of debris within the cloud as a function of time and of the spatial and temporal distribution of radioactivity deposited on the ground.

Theoretical investigations into the formation of debris particles to determine the particle size distribution for various yields and its evolution with time are planned. A continued effort will be made toward understanding the chemical composition of the debris particles and manipulation of the wettability of the particle surfaces to affect nucleation.

Additional work is needed to more realistically describe rainout. Among the problems to be studied are what fraction of debris particles can serve as condensation nuclei in a given precipitation system and how these particles compete with the natural condensation nuclei. If a large number of small particles result from a detonation, they would attach themselves to natural aerosol particles by virtue of their Brownian motion, and the removal of the contaminated natural aerosol particles must then be considered.

The calculation of dry deposition can be improved by including the effect of wind shear on the traveling debris system. Another problem is the efficiency by which these particles attach to the earth's surface. Future work into this problem area is planned as well as an assessment of the global effects of wet and dry deposition.

Fohl and Zalay[45] suggested that the height of rise of two buoyant fireballs released simultaneously and in close proximity will be decreased by their mutual interaction. Further and more fundamental work is needed to evaluate and predict this phenomenon and to assess its implications on the scavenging of debris.

In order to more effectively assess the consequences of the rainout problem, a climatological study for areas of interest is planned. Such information as the depth of convection cell size, the fraction of time that precipitating systems are present, and the type of flow above precipitating systems coupled with improved rainout estimates, can be useful for military planning.

Acknowledgments

The authors wish to thank Theodore W. Stullich for programming the microphysical scavenging calculations.

The work reported in this paper was performed in part under the auspices of the U.S. Atomic Energy Commission and in part under the sponsorship of DNA Contract IACRO-73-814, Subtask Number W99QAXTD87 (Precipitation Scavenging).

References

1. J.E. Knox, T.V. Crawford, and W.K. Crandall, Potential Exposures from Low-Yield Free Air Bursts, Lawrence Livermore Laboratory, Rept. UCRL-51164 (1971).
2. G. Conner and J. Phillips, Radiological Hazard Due to Rain Through a Nuclear Cloud, unpublished Defense Nuclear Agency study (Confidential).
3. N.H. Fletcher, "Size Effect in Heterogeneous Nucleation," J. Chem. Phys. 29 572 and 31, 1136 (1958).
4. S. Twomey, "Experimental Test of the Volmer Theory of Heterogeneous Nucleation," J. Chem. Phys. 30 941 (1959).
5. S. Glasstone, The Effects of Nuclear Weapons, U.S. Atomic Energy Commission, Washington, D.C. (1962).
6. T.V. Crawford, A Computer Program for Calculating the Atmospheric Dispersion of Large Clouds, Lawrence Livermore Laboratory, Rept. UCRL-50179 (1966).
7. Local Fallout from Nuclear Test Detonations, Stanford Research Institute, Menlo Park, Calif., Rept. DASA-12-51/NOL-TR-65 (1965), Vol. V, "Transport and Distribution of Local (Early) Fallout from Nuclear Weapons Tests" (Title U, Report SRD).
8. H.L. Crutcher, Upper Wind Statistics of the Northern Hemisphere, Chief of Naval Operations, Washington, D.C., Rept. NAVAER-50-1C-535 (1959).
9. E.M. Wilkins, New Applications of Atmospheric Turbulence and Diffusion Theory, Ling-Temco-Vought, Dallas, Tex., Rept. 0-7100/312-19 (1963).
10. H.W. Ellsaesser, "A Climatology of Epsilon (Atmospheric Dissipation)," Mon. Weather Rev. 97, 415 (1969).
11. A.I. Weinstein and L.G. Davis, A Parameterized Numerical Model of Cumulus Convection, Department of Meteorology, the Pennsylvania State University, University Park, Report No. 11 to the National Science Foundation, NSF Grant GA-13818, December 1967. Revised May 1968.
12. B.B. Hicks, "Nucleation and the Wet Removal of Fallout," J. of Applied Met. 5 (1966).
13. K. Stewart, "The Condensation of a Vapour to an Assembly of Droplets or Particles," Trans. Farady Soc. 52, 161 (1956).
14. M.W. Nathaus, R. News, W.D. Holland, and P.A. Benson, "Particle Size Distribution in Clouds from Nuclear Air Bursts," J. of Geophysical Res. 75, 7559 (1970).
15. A.C. Chamberlain, Aspects of Travel and Deposition of Aerosol and Vapor Clouds, Atomic Energy Research Establishment, Rept. AERE-HP/R-1261 (1953).
16. W.G.N. Slinn and J.M. Hales, "A Reevaluation of the Role of Thermophoresis as a Mechanism of In- and Below-Cloud Scavenging," J. Atmos. Sci. 8 1465 (1971).
17. A.L. Williams, Diffusiophoretic Forces Between Juxtaposed Atmospheric Particles, Ph.D. Thesis, University of Missouri at Rolla (1972).

18. B. P. LeClair, A. E. Hamielec, and H. R. Pruppacher, "A Numerical Study of the Drag on a Sphere at Low and Intermediate Reynolds Numbers," J. Atmos. Sci. 27, 308 (1970).
19. R. Gunn and G. D. Kinzer, "The Terminal Velocity of Fall for Water Droplets in Stagnant Air," J. Met. 6, 243 (1959).
20. I. Langmuir, "The Production of Rain by a Chain Reaction in Cumulus Clouds at Temperatures Above Freezing," J. Met. 5, 175 (1948).
21. A. C. Best, "The Size Distribution of Rain Drops," Quart. J. R. Met. Soc. 76, 16 (1950).
22. B. J. Mason and J. B. Andrews, "Drop-Size Distributions from Various Types of Rain," Quant. J. R. Met. Soc. 86, 346 (1960).
23. R. Heft, "The Characterization of Radioactive Particles from Nuclear Weapons Tests," Radionuclides in the Environment (American Chemical Society, Washington, D. C., 1970).
24. D. T. Liney and P. Murry, "Surface Energy of Solid Oxides and Carbides," J. Am. Ceram. Soc. 31 (11), 363-372 (1956).
25. L. Shartsis, S. Spnner, and A. W. Smock, "Surface Tension of Compositions in the Systems PbO-SiO_2," J. Am. Ceram. Soc. 31, (1) 23-27 (1948).
26. F. H. Norton, W. D. Kingery, G. Economos, and M. Humenik, Study of Metal-Ceramic Interactions at Elevated Temperatures, U. S. Atomic Energy Commission, Rept. NYO-3144 (1953).
27. V. K. Semenchenko, Surface Phenomena in Metals and Alloys (Addison-Wesley, Reading, Mass., 1962).
28. Metals Handbook, Vol. I (American Society for Metals, Metals Park, Ohio, 1961).
29. W. A. Zisman, Advances in Chemistry, Series 43 (American Chemical Society, Washington, D. C., 1964).
30. J. T. Davies and E. K. Rideal, Interfacial Phenomena (Academic Press, N. Y., 1961).
31. R. Defay, I. Prigogine, and A. Bellemans, Surface Tension and Adsorption (John Wiley, New York, 1966).
32. E. F. Hare, E. G. Shafrin, and W. A. Zisman, "Properties of Films of Adsorbed Fluorinated Acids," J. Phys. Chem. 58, 236 (1954).
33. F. Schulman and W. A. Zisman, "The Spreading of Liquids in Low-Energy Surfaces: V. Perfluorodecanoic Acid Monolayers," J. Colloid Sci. 7, 465 (1952).
34. K. C. D. Hickman and W. A. Torpey, Ind. Eng. Chem. 46, 1446 (1954).
35. V. K. LaMer, Retardation of Evaporation by Monolayers (Academic Press, New York, 1961).
36. T. Alty and C. A. MacKay, "The Accommodation Coefficient and the Evaporation Coefficient of Water," Proc. Roy. Soc., Series A 149, 104 (1935).
37. T. Young, Phil. Trans. Roy. Soc. 95, 65 (1805).

38. R. E. Johnson, "Conflicts Between Gibbsian Thermodynamics and Recent Treatments of Interfacial Energies in Solid-Liquid-Vapor Systems," J. Phys. Chem. 63, 1655 (1959).
39. A. Dupré, Théorie Mécanique de la Chaleur, Paris (1869).
40. W. A. Cooper and W. H. Nuttall, J. Agr. Sci. 7, 219 (1915).
41. W. D. Harkins, "Surface Films of Fatty Acids, Alcohols, and Esters," Chem. Rev. 29, 385 (1941).
42. J. E. Welch, F. H. Harlow, J. P. Shannon, and B. J. Daly, The MAC Method, Los Alamos Scientific Laboratory, New Mexico, Rept. LA-3425 (1965).
43. A. A. Amsden, The Particle-In-Cell Method for the Calculation of the Dynamics of Compressible Fluids, Los Alamos Scientific Laboratory, New Mexico, Rept. LA-3466 (1966).
44. R. C. Sklawew, A. J. Fabrick, and J. E. Prager, A Particle-In-Cell Method for Numerical Solution of the Atmospheric Diffusion Equation, and Application to Air Pollution Problems, Systems, Science and Software, La Jolla, California, Rept. 3SR-844 (1971).
45. T. Fohl and A. D. Zalay, Vortex Ring Model of Single and Multiple Cloud Rise, Defense Nuclear Agency, Rept. DNA-2945F (1972).

Printed in USA. Available from the National Technical Information Center, National Bureau of Standards, U.S. Department of Commerce, Springfield, Virginia 22151
Price: Printed Copy $3.00; Microfiche $0.95.